Supporting Information

Fourier Transform to Analyze Reaction–Diffusion Dynamics in a Microsystem

André Estévez-Torres,[a] Thomas Le Saux,[a] Charlie Gosse,[b],* Annie Lemarchand,[c] Anne Bourdoncle,[a] Ludovic Jullien[a],*

[a] *A. Estévez-Torres, T. Le Saux, A. Bourdoncle, L. Jullien,*
École Normale Supérieure, Département de Chimie,
UMR CNRS-ENS-UPMC Paris6 PASTEUR 8640,
24, rue Lhomond, 75231 Paris Cedex 05, France
Fax: (+33) 1 44 32 33 25, E-mail: Ludovic.Jullien@ens.fr, http://www.chimie.ens.fr
[b] *C. Gosse,*
Laboratoire de Photonique et de Nanostructures, LPN-CNRS,
Route de Nozay, 91460 Marcoussis, France
[c] *A. Lemarchand,*
Université Pierre et Marie Curie Paris6,
Laboratoire de Physique Théorique de la Matière Condensée, UMR CNRS 7600,
4, place Jussieu, 75252 Paris Cedex 05, France

- Theoretical derivation of the expression of the Fourier transform of the concentrations $R(x, y)$ and $P(x, y)$ with respect to y;
- Extraction of the dynamic parameters from the stationary reaction-migration-diffusion pattern of the fluorescence signal;
- Independent extraction, by fluorescence spectroscopy, of the thermodynamic constant K and rate constants k_1 and k_2.
- Independent evaluation of the diffusion coefficients, d_R and d_P, and of the velocities, v_R and v_P, of the oligonucleotides;
- Experimental constraints to retrieve the kinetic information from the reaction-migration-diffusion pattern.

Theoretical derivation of the expression of the Fourier transform of the concentrations $R(x,y)$ and $P(x,y)$ with respect to y

We consider that the reactive system contains three species, $\mathbf{R}$, $\mathcal{R}$, and $\mathbf{P}$, which are involved in the chemical reaction:

$$\mathbf{R} + \mathcal{R} \quad \underset{k_2}{\overset{k_1}{\rightleftharpoons}} \quad \mathbf{P} \tag{1}$$

where k_1 and k_2 designate the rate constants associated to the forward and backward reactions, respectively. We suppose that the reactant $\mathcal{R}$ is in great excess with respect to $\mathbf{R}$ and $\mathbf{P}$ ($\mathcal{R} \gg R$ and $\mathcal{R} \gg P$) and has a constant uniform concentration. We correspondingly introduce $k_1\mathcal{R}$ as an effective forward rate constant. Under such conditions, reaction (1) reduces to the simple two-state exchange process between $\mathbf{R}$ and $\mathbf{P}$

$$\mathbf{R} \quad \underset{k_2}{\overset{k_1\mathcal{R}}{\rightleftharpoons}} \quad \mathbf{P} \tag{2}$$

which apparent thermodynamic constant is $K' = \frac{k_1[\mathcal{R}]}{k_2}$.

To calculate the stationary reaction-migration-diffusion pattern described in the Main Text, we assume that the $\mathbf{R}$ and $\mathbf{P}$ motion occurs in a two-dimensional (2D) medium defined by ($0 \leq x \leq L, -\infty < y < +\infty$). This medium is submitted to a uniform constant electric field $\overrightarrow{E} = E\overrightarrow{u_x}$, where $\overrightarrow{u_x}$ is the unit vector along x. The diffusion coefficients of species $\mathbf{R}$ and $\mathbf{P}$ are respectively denoted d_R and d_P and their velocities (along the x-axis) v_R and v_P. $\overrightarrow{E}$ is chosen to impose the migration of the averaged species {$\mathbf{R}$,$\mathbf{P}$} in the direction of increasing x. Considering at the (x=0,y=0) origin a {$\mathbf{R}$,$\mathbf{P}$} source associated to the equilibrium conditions $R(0,0)$ and $P(0,0)$, we look for stationary concentrations profiles, $R(x,y)$ and $P(x,y)$, obeying the following partial differential equations:

$$-v_R\frac{\partial R(x,y)}{\partial x} + d_R\left[\frac{\partial^2 R(x,y)}{\partial x^2} + \frac{\partial^2 R(x,y)}{\partial y^2}\right] - k_1\mathcal{R}R(x,y) + k_2P(x,y) = 0 \tag{3}$$

$$-v_P\frac{\partial P(x,y)}{\partial x} + d_P\left[\frac{\partial^2 P(x,y)}{\partial x^2} + \frac{\partial^2 P(x,y)}{\partial y^2}\right] + k_1\mathcal{R}R(x,y) - k_2P(x,y) = 0 \tag{4}$$

After Fourier transform along y, Eqs. (3,4) lead to

$$\frac{\partial^2 \tilde{R}(x,q)}{\partial x^2} - \frac{v_R}{d_R}\frac{\partial \tilde{R}(x,q)}{\partial x} - \left(q^2 + \frac{k_1 \mathcal{R}}{d_R}\right)\tilde{R}(x,q) = -\frac{k_2}{d_R}\tilde{P}(x,q) \quad (5)$$

$$\frac{\partial^2 \tilde{P}(x,q)}{\partial x^2} - \frac{v_P}{d_P}\frac{\partial \tilde{P}(x,q)}{\partial x} - \left(q^2 + \frac{k_2}{d_P}\right)\tilde{P}(x,q) = -\frac{k_1 \mathcal{R}}{d_P}\tilde{R}(x,q) \quad (6)$$

where $\tilde{R}(x,q) = 1/\sqrt{2\pi}\int_{-\infty}^{\infty} R(x,y)e^{-iqy}dy$ and $\tilde{P}(x,q) = 1/\sqrt{2\pi}\int_{-\infty}^{\infty} P(x,y)e^{-iqy}dy$.

We restrict our analysis to a regime where diffusion along x is negligible with respect to migration:[1]

$$\frac{\partial^2 \tilde{R}}{\partial x^2} \ll \frac{v_R}{d_R}\frac{\partial \tilde{R}}{\partial x} \quad (7)$$

$$\frac{\partial^2 \tilde{P}}{\partial x^2} \ll \frac{v_P}{d_P}\frac{\partial \tilde{P}}{\partial x} \quad (8)$$

Thus, Eqs.(5,6) become:

$$\frac{\partial \tilde{R}(x,q)}{\partial x} = -\frac{1}{v_R}(d_R q^2 + k_1 \mathcal{R})\tilde{R}(x,q) + \frac{1}{v_R}k_2 \tilde{P}(x,q) \quad (9)$$

$$\frac{\partial \tilde{P}(x,q)}{\partial x} = \frac{1}{v_P}k_1 \mathcal{R}\tilde{R}(x,q) - \frac{1}{v_P}(d_P q^2 + k_2)\tilde{P}(x,q) \quad (10)$$

Eventually, we introduce the variables $\kappa_1 = \frac{k_1 \mathcal{R}}{v_R}$, $\kappa_1' = \kappa_1 \frac{v_R}{v_P}$, $\kappa_2 = \frac{k_2}{v_P}$, $\kappa_2' = \kappa_2 \frac{v_P}{v_R}$, $\delta_R = \frac{d_R}{v_R}$, and $\delta_P = \frac{d_P}{v_P}$ to simplify the Eqs.(9,10) expressions:

$$\frac{\partial \tilde{R}(x,q)}{\partial x} = -(\delta_R q^2 + \kappa_1)\tilde{R}(x,q) + \kappa_2' \tilde{P}(x,q) \quad (11)$$

$$\frac{\partial \tilde{P}(x,q)}{\partial x} = \kappa_1' \tilde{R}(x,q) - (\delta_P q^2 + \kappa_2)\tilde{P}(x,q) \quad (12)$$

The latter linear system admits solutions in the form:

$$\tilde{R}(x,q) = R_+ e^{\lambda_+ x} + R_- e^{\lambda_- x} \quad (13)$$

$$\tilde{P}(x,q) = P_+ e^{\lambda_+ x} + P_- e^{\lambda_- x} \quad (14)$$

where the eigenvalues obey:

$$\lambda_\pm = -\frac{1}{2}\left[(\kappa_1 + \kappa_2) + (\delta_R + \delta_P)q^2\right] \pm \frac{1}{2}\sqrt{\left[(\kappa_1 + \kappa_2) + (\delta_R - \delta_P)\,q^2\right]^2 + 4(\delta_P - \delta_R)q^2\kappa_2} \quad (15)$$

[1]The following relations correspond to the conditions: $\frac{L_x v_R}{d_R} \gg 1$ and $\frac{L_x v_P}{d_P} \gg 1$ where L_x designate the image length along the x-axis. Such conditions were always fulfilled in the present study.

and where the amplitudes are given by:

$$R_+ = \frac{1}{(\lambda_+ - \lambda_-)}\left[-(\delta_R q^2 + \kappa_1 + \lambda_-)\tilde{R}(0,q) + \kappa_2'\tilde{P}(0,q)\right] \tag{16}$$

$$R_- = \frac{1}{(\lambda_+ - \lambda_-)}\left[(\delta_R q^2 + \kappa_1 + \lambda_+)\tilde{R}(0,q) - \kappa_2'\tilde{P}(0,q)\right] \tag{17}$$

$$P_+ = \frac{1}{(\lambda_+ - \lambda_-)}\left[\kappa_1'\tilde{R}(0,q) - (\delta_P q^2 + \kappa_2 + \lambda_-)\tilde{P}(0,q)\right] \tag{18}$$

$$P_- = \frac{1}{(\lambda_+ - \lambda_-)}\left[-\kappa_1'\tilde{R}(0,q) + (\delta_P q^2 + \kappa_2 + \lambda_+)\tilde{P}(0,q)\right] \tag{19}$$

$\tilde{R}(0,q)$ and $\tilde{P}(0,q)$ are here the Fourier transforms of the $R(0,y)$ and $P(0,y)$ initial conditions, respectively.

Finally, Eqs.(16–19) can be transformed according to the following. First, we introduce $\tilde{\mathcal{G}}(0,q)$, a q-dependent function which reflects the geometry of the channel at the entry of the measurement chamber : $\tilde{\mathcal{G}}(0,q) = \frac{\tilde{R}(0,q)}{\tilde{R}(0,0)} = \frac{\tilde{P}(0,q)}{\tilde{P}(0,0)}$. By doing so, we assume that the normalized Fourier transform of the concentration profile at $x = 0$ is independent on the solute nature, which could be verified experimentally.[2] Second, we make use of the equilibrium condition before injection, $K' = P(0,0)/R(0,0)$. Eqs.(16–19) become Eqs.(20–23):

$$R_+ = -\frac{1}{(\lambda_+ - \lambda_-)}(\delta_R q^2 + \lambda_-)\tilde{\mathcal{G}}(0,q)\frac{1}{1+K'}C_0 \tag{20}$$

$$R_- = \frac{1}{(\lambda_+ - \lambda_-)}(\delta_R q^2 + \lambda_+)\tilde{\mathcal{G}}(0,q)\frac{1}{1+K'}C_0 \tag{21}$$

$$P_+ = -\frac{1}{(\lambda_+ - \lambda_-)}(\delta_P q^2 + \lambda_-)\tilde{\mathcal{G}}(0,q)\frac{K'}{1+K'}C_0 \tag{22}$$

$$P_- = \frac{1}{(\lambda_+ - \lambda_-)}(\delta_P q^2 + \lambda_+)\tilde{\mathcal{G}}(0,q)\frac{K'}{1+K'}C_0 \tag{23}$$

where $C_0 = R(0,0) + P(0,0)$ designates the total concentration in $\mathbf{R}$ and $\mathbf{P}$ in the loaded sample.

[2]In the present microsystem, the initial condition is not taken at the entry of the measurement chamber but at the abscissa where the electric field becomes constant.[1] Thus $\tilde{\mathcal{G}}(0,q)$ reflects not only the shape of the channel, but also some broadening by migration, due to out-of-axis electric fields between the injection nozzle and the zone of homogeneous velocity, as well as by molecular diffusion. We demonstrated in a previous report that the width of the corresponding initial condition was gaussian with a typical 60 μm half-width that did not depend on the solute, whatever the investigated sample (oligonucleotide or dsDNA).[1] In the case where the geometry of the initial profiles of $\mathbf{R}$ and $\mathbf{P}$ would not be identical, it would be necessary to keep the $\tilde{R}(0,q)$ and $\tilde{P}(0,q)$ terms in the amplitudes expressions of the exponential terms.

Extraction of the dynamic parameters from the stationary reaction-migration-diffusion pattern of the fluorescence signal

Theoretical expression of the stationary reaction-migration-diffusion pattern of the fluorescence signal

Introducing $\mathcal{Q}_R$ and $\mathcal{Q}_P$ as, respectively, the **R** and **P** brightness, the theoretical q-dependence of $\tilde{\mathcal{F}}(x,q)$, the stationary reaction-migration-diffusion pattern observed by fluorescence video microscopy, can be derived from Eqs.(13–14) and Eqs.(20–23):

$$\tilde{\mathcal{F}}(x,q) = \mathcal{F}_+ e^{\lambda_+ x} + \mathcal{F}_- e^{\lambda_- x} \tag{24}$$

with the decays λ_+ and λ_- given by Eqs.(15) and the amplitudes $\mathcal{F}_+$ and $\mathcal{F}_-$ by:

$$\mathcal{F}_+ = -\frac{1}{(\lambda_+ - \lambda_-)} \left[(\delta_R q^2 + \lambda_-)\mathcal{Q}_R \frac{1}{1+K'} + (\delta_P q^2 + \lambda_-)\mathcal{Q}_P \frac{K'}{1+K'} \right] \tilde{\mathcal{G}}(0,q) C_0 \tag{25}$$

$$\mathcal{F}_- = \frac{1}{(\lambda_+ - \lambda_-)} \left[(\delta_R q^2 + \lambda_+)\mathcal{Q}_R \frac{1}{1+K'} + (\delta_P q^2 + \lambda_+)\mathcal{Q}_P \frac{K'}{1+K'} \right] \tilde{\mathcal{G}}(0,q) C_0. \tag{26}$$

In practice, to correct from any illumination homogeneity or photobleaching, the $\tilde{\mathcal{F}}(x,q)$ pattern is normalized by the zeroth mode $\tilde{\mathcal{F}}(x,0)$ [1] which is equal to $(\mathcal{Q}_R \frac{1}{1+K'} + \mathcal{Q}_P \frac{K'}{1+K'}) C_0$ (see Eqs. (15) and (24–26)). We thus have:

$$\frac{\tilde{\mathcal{F}}(x,q)}{\tilde{\mathcal{F}}(x,0)} = \mathcal{F}_+^{norm} e^{\lambda_+ x} + \mathcal{F}_-^{norm} e^{\lambda_- x} \tag{27}$$

with

$$\mathcal{F}_+^{norm} = -\frac{1}{(\lambda_+ - \lambda_-)} \left[(\delta_R q^2 + \lambda_-)\mathcal{I}_R + (\delta_P q^2 + \lambda_-)\mathcal{I}_P \right] \tilde{\mathcal{G}}(0,q) \tag{28}$$

$$\mathcal{F}_-^{norm} = 1 - \mathcal{F}_+^{norm} \tag{29}$$

We introduced here the respective **R** and **P** fractionary fluorescence intensity:

$$\mathcal{I}_R = \frac{1}{1+QK'} \tag{30}$$

$$\mathcal{I}_P = \frac{QK'}{1+QK'} \tag{31}$$

and the relative brightness of **P** with regard to **R** : $Q = \frac{\mathcal{Q}_P}{\mathcal{Q}_R}$.

Extraction of the dynamic parameters

Seven parameters characterize the association dynamics between **R** and $\mathcal{R}$: d_R, d_P, v_R, v_P, $k_1\mathcal{R}$, k_2,[3] and Q. We assume that d_R and v_R have first been measured with the same microsystem during a preliminary experiment performed by injecting **R** only.[1] Thus five parameters, d_P, v_P, $k_1\mathcal{R}$, k_2, and Q, remain to be determined from analyzing the stationary reaction-migration-diffusion pattern of the fluorescence signal. As shown in the following, the four first ones can be extracted from the spatial analysis of the $\tilde{\mathcal{F}}(x,q)$ collection whereas Q can be obtained from the corresponding amplitude analysis. From an experimental point of view, analyzing the decay rates is particularly advantageous since the spatial dependence of $\tilde{\mathcal{F}}(x,q)$ does not depend on the shapes of the initial concentration profiles $\tilde{R}(0,q)$ and $\tilde{P}(0,q)$ (contained in the $\tilde{\mathcal{G}}(0,q)$ function).

The spatial analysis of the collection of the $\tilde{\mathcal{F}}(x,q)$ terms provides the q-dependence of the eigenvalues λ_+ and λ_-[4] from which κ_1, κ_2, and δ_P can be extracted (δ_R has been measured in a preliminary experiment).[5] Data are subsequently analyzed in the following way:

- Beyond the relaxation time $\tau_\chi = \frac{1}{k_1\mathcal{R}+k_2}$, the reactive system submitted to the reaction (1) behaves as if it would contain one averaged species {**R**,**P**} only. At low enough applied voltage u, the velocity along the x-axis of the latter, $v^u_{\{R,P\}} = \frac{1}{1+K'}v^u_R + \frac{K'}{1+K'}v^u_P$, can be independently measured by recording beyond $x_\chi = v^u_{\{R,P\}}\tau_\chi$ the introduction of the fluorescent front of the mixture into the analysis chamber. Then the velocity $v_{\{R,P\}} = \frac{1}{1+K'}v_R + \frac{K'}{1+K'}v_P$ is deduced from the actual voltage U during the experiment as $v_{\{R,P\}} = \frac{U}{u}v^u_{\{R,P\}}$ (See Figure S-6 in reference [1]);

- As expressed above, $v_{\{R,P\}}$ depends on v_R, v_P, and K'. The ratio $\frac{\kappa_1}{\kappa_2} = \frac{v_P}{v_R}K'$ provides a second independent observable linking v_R, v_P, and K'. v_R being known

[3] K' can be calculated from k_1 and k_2.

[4] From an experimental point of view, it is essential to collect a large set of $\lambda_+(q)$ and $\lambda_-(q)$ to reliably extract κ_1, κ_2, δ_R, and δ_P. In particular, it is important to reach an asymptotic regime dominated by diffusion only (*vide supra*). It can either be the one of "slow" or "fast" chemistry. In the investigated experimental system, we decreased the applied electric field to be able to reliably measure λ_+ and λ_- for the smallest q values associated to a regime of fast exchange between **R** and **P**.

[5] This conclusion can be evidenced by considering the q-dependence of $\lambda_+ + \lambda_- = -(\kappa_1+\kappa_2) - (\delta_R + \delta_P)q^2$ and of $\frac{\lambda_+\lambda_-}{q^2} = (\kappa_1\delta_P + \kappa_2\delta_R) + (\delta_R\delta_P)q^2$ easily derived from Eqs.(15).

(*vide supra*), v_P and K' can be obtained;

- k_1 is derived from κ_1 by using the value of v_R. Then k_2, is extracted from the values of K' and $k_1\mathcal{R}$;

- d_P is eventually obtained from δ_P and v_P.

Once d_R, d_P, v_R, v_P, $k_1\mathcal{R}$, and k_2 have been obtained, Q can be extracted from the ratio $\frac{\mathcal{F}_{+,norm}(q)}{\mathcal{F}_{-,norm}(q)}$, i. e. the amplitude analysis of the collection of the $\tilde{\mathcal{F}}(t,q)$ terms.

Independent extraction, by fluorescence spectroscopy, of the thermodynamic constant K and rate constants k_1 and k_2

Fluorescence measurements were performed on a LPS 220 spectrofluorimeter (Photon Technology International, Birmingham, NJ) in 25/50 mM NaOH/Hepes, 1.25/5 mM $Mg(OH)_2$/Hepes buffer, pH 7.5, supplemented with 10 μg/mL sonicated DNA salmon sperm, to prevent oligonucleotide adsorption, and 0.1% (w/w) PDMA (T = 20°C). A quartz cuvette with a 1 cm optical path was used; excitation and emission wavelengths were respectively set at 587 and 612 nm with a bandwidth of 4 nm. After each experiment, the cuvette was cleaned for 15 minutes with a 1% (v/v) Hellmanex soap (Hellma, Mulheïm, Germany) in an ultrasonic bath.

Thermodynamic measurements

400 μL of 50 nM tex-9 were equilibrated at 20°C. The decrease in fluorescence intensity, associated to the hybridization process, was recorded while increasing concentrations of M100 were added at constant tex-9 concentration (Figure 1S). Data were then analyzed on the basis of reaction (1), for which the following formula can be easily obtained:

$$\frac{I_{eq}}{I_0} = 1 - \frac{1}{2}(1-\mathcal{Q})\left\{\left(1+\xi+\frac{1}{KR_0}\right) - \sqrt{\left(1+\xi+\frac{1}{KR_0}\right)^2 - 4\xi}\right\}, \qquad (32)$$

where I_{eq} is the fluorescence intensity at equilibrium when $\xi = \frac{\mathcal{R}}{R_0}$ equivalents of species $\mathcal{R}$ (ie M100) have been added, I_0 the intensity at the beginning of the experiment, R_0 the initial concentration in tex-9, and $\mathcal{Q}$ the relative brightness of the duplex with regards to the free 9mer. R_0 being known, we extract K and $\mathcal{Q}$ by a least-squares fit. Results are displayed in Figure 1S.

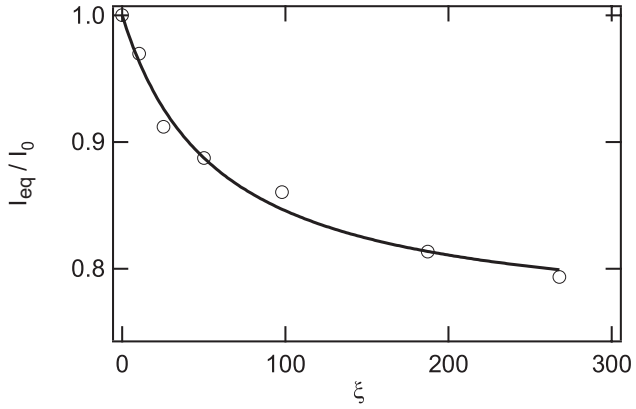

Figure 1S. Normalized fluorescence intensity at equilibrium *vs.* the number of equivalents of M100 added to a 50 nM tex-9 solution. The solid line corresponds to the fit according to Eq.(32). We extracted $K = 3.4 \pm 0.6 \times 10^5$ and $\mathcal{Q} = 0.75 \pm 0.02$.

Kinetic measurements

Using a RX2000 rapid kinetic stopped flow accessory (Applied Photophysics, Leatherhead, UK), two 200 μL solutions, A and B, were mixed with typical dead times of 100 ms and the fluorescence intensity was recorded over time at either 10 or 100 Hz. In association experiments, solution A contained tex-9 and solution B M100 (final concentrations 50 nM and 10 μM, respectively). In dissociation experiments, solution A contained an equilibrated mixture of tex-9+M100 (final concentrations 50 nM and 10 μM, respectively) and solution B an unlabeled oligonucleotide having a much stronger affinity for M100 than tex-9 (U13 – final concentration 50 μM).

Model for association experiments

The association reaction (1) reduces to (2) when $\mathcal{R}$ is in excess with respect to $\mathbf{R}$. The kinetic law associated to reaction (2) in a homogeneous solution is

$$\frac{dR(t)}{dt} = -k_1 \mathcal{R} R(t) + k_2 P(t). \tag{33}$$

Considering the initial condition R_0 and the conservation of matter, $R(t) + P(t) = R_0$, Eq. (33) yields the solution:

$$R(t) = R_{eq} + [R_0 - R_{eq}] e^{-t/\tau}, \tag{34}$$

where R_{eq} is the concentration of $\mathbf{R}$ at equilibrium and $\tau = (k_1\mathcal{R} + k_2)^{-1}$. Eq.(34) can be eventually used to derive the temporal dependence of the normalized fluorescence intensity $I(t)/I_0$:

$$\frac{I(t)}{I_0} = \frac{I_{eq}}{I_0} + \left(1 - \frac{I_{eq}}{I_0}\right) e^{-t/\tau} \tag{35}$$

where

$$\frac{I_{eq}}{I_0} = \frac{1 + K'\mathcal{Q}}{1 + K'}. \tag{36}$$

Model for dissociation experiments

To determine k_2, we performed displacement experiments in which the unlabeled oligonucleotide U13 ($\mathbf{R}_{NF}$) hybridized with M100 ($\mathcal{R}$) and took the place of tex-9 ($\mathbf{R}$) in the fluorescent duplex $\mathbf{P}$ to form a much more stable non-fluorescent duplex ($\mathbf{P}_{NF}$). The corresponding kinetic scheme can be written:

$$\mathbf{P} \underset{k_1}{\overset{k_2}{\rightleftharpoons}} \mathbf{R} + \mathcal{R} \tag{37}$$

$$\mathbf{R}_{NF} + \mathcal{R} \rightleftharpoons \mathbf{P}_{NF} \tag{38}$$

When the concentrations are chosen to make the dissociation of the fluorescent duplex $\mathbf{P}$ rate-limiting with regards to the subsequent formation of non-fluorescent duplex $\mathbf{P}_{NF}$, the time dependence of the $\mathbf{R}$ concentration is given by:

$$R(t) = R_{eq} + (R_0 - R_{eq})e^{-k_2 t} \tag{39}$$

where R_0 and R_{eq} now designate the initial and final equilibrium concentrations of species $\mathbf{R}$ during dissociation experiments. The corresponding temporal evolution of the normalized fluorescence intensity $I(t)/I_0$ is:

$$\frac{I(t)}{I_0} = \frac{I_{eq}}{I_0} + \left(1 - \frac{I_{eq}}{I_0}\right) e^{-k_2 t} \tag{40}$$

where

$$\frac{I_{eq}}{I_0} = \frac{R_{eq} + \mathcal{Q}P_{eq}}{R_0 + \mathcal{Q}P_0}. \tag{41}$$

Analysis of the experimental results

The results of the association and dissociation experiments are displayed in Figure 2Sa and 2Sb, respectively. k_2 is first extracted from fitting the experimental data in Figure 2Sb. $k_1\mathcal{R}$ (or similarly k_1) is subsequently derived using the τ value extracted from the temporal dependence displayed in Figure 2Sa. Eventually, the relative brightness $\mathcal{Q}$ is obtained from analyzing the amplitude of the temporal dependence in Figure 2Sa, introducing the value of $K = \frac{k_1}{k_2}$ in Eq.(36).

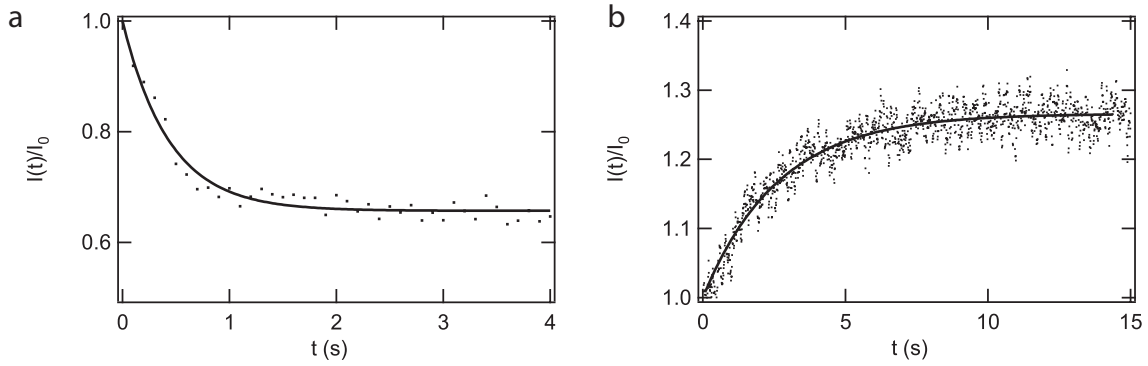

Figure 2S. Normalized fluorescence intensity for the association (a) and dissociation (b) of 50 nM tex-9 + 10 μM M100. Solid lines correspond to monoexponential fits according to Eqs (35) and (40) respectively. We extracted $k_1\mathcal{R} = 1.9 \pm 0.1$ s^{-1} ($k_1 = 1.9 \pm 0.1\ 10^5$ M^{-1}s^{-1}), $k_2 = 0.42 \pm 0.01$ s^{-1} ($\tau = 2.4 \pm 0.1$ s^{-1}), and $\mathcal{Q} = 0.76$.

Independent evaluation of the diffusion coefficients, d_R and d_P, and of the velocities, v_R and v_P, of the oligonucleotides

The diffusion coefficient and the velocity of tex-9 (**R**) can directly be measured as described in reference [1], using the protocol established for a pure species. The experiment was performed at 20°C in 25/50 mM NaOH/Hepes, 1.25/5 mM $Mg(OH)_2$/Hepes buffer, pH 7.5. A 1 μM oligonucleotide sample was injected in the analysis chamber upon applying a 300 V voltage drop. We extracted a diffusion coefficient and a mobility equal to 153 $\pm$ 10 $\mu m^2 s^{-1}$ and 20 $\pm$ 2 10^{-9} $m^2 V^{-1} s^{-1}$, respectively.

In contrast, the diffusion coefficient and the velocity of the duplex (**P**), resulting from the tex-9 hybridization with M100 ($\mathcal{R}$), cannot be directly obtained at 20°C and at micromolar concentrations using the reference [1] protocol established for a non-reactive binary mixture. Indeed kinetics is precisely present under such experimental conditions. Alternatively, we relied on measurements performed on the duplex formed by tex-9 hybridization with C100, the M100 analog bearing the perfect matched sequence. The tex-9/C100 duplex is more stable than the tex-9/M100 one and it does not dissociate at the timescale of the experiment; consequently, we can now apply the protocol reported in reference [1] for a binary mixture to extracted the parameters sought for. Note that mispairing in tex-9/M100 is not expected to introduce any significant change of diffusion coefficient or velocity with regards to results that could be obtained on tex-9/C100. We injected at 20°C a mixture of tex-9 and C100, 1 and 10 μM respectively, and applied the binary mixture biexponential fitting procedure while setting the tex-9 diffusion coefficient at 153 $\pm$ 10 $\mu m^2 s^{-1}$. From this experiment, the **P** diffusion coefficient and mobility were respectively evaluated to 40 $\pm$ 4 $\mu m^2 s^{-1}$ and 20 $\pm$ 2 10^{-9} $m^2 V^{-1} s^{-1}$.

Experimental constraints to retrieve the kinetic information from the reaction-migration-diffusion pattern

The expression of the eigenvalues given in Eqs.(15) can be much simplified according to the relative values of two apparent relaxation rates: $(\kappa_1+\kappa_2)$ that characterize the species reactivity and $(\delta_R-\delta_P)q^2$ that governs the diffusive behavior difference between **R** and **P** at the spatial scale q.

- If $(\kappa_1+\kappa_2) \ll (\delta_R-\delta_P)q^2$, diffusion dominates chemistry for relaxation towards equilibrium at the spatial scale q. The mixture seems non reactive; its components **R** and **P** diffuse independently with apparent diffusion coefficients δ_R and δ_P, respectively. Introducing $K'=\frac{k_1}{k_2}$, the apparent thermodynamic constant associated to the reaction (2), we have $\tilde{R}(x,q) \simeq \tilde{\mathcal{G}}(0,q)\frac{1}{1+K'}C_0\exp(-\delta_R q^2 x)$ and $\tilde{P}(x,q) \simeq \tilde{\mathcal{G}}(0,q)\frac{K'}{1+K'}C_0\exp(-\delta_P q^2 x)$ at zeroth order;

- If $(\kappa_1+\kappa_2) \gg (\delta_R-\delta_P)q^2$, chemistry dominates diffusion for relaxation towards equilibrium at the spatial scale q: The reactive mixture behaves as a single component with a $\frac{1}{2}(\delta_R+\delta_P)$ apparent diffusion coefficient. $\tilde{R}(x,q) \simeq \tilde{\mathcal{G}}(0,q)\frac{1}{1+K'}C_0\exp[-\frac{1}{2}(\delta_R+\delta_P)q^2x]$ and $\tilde{P}(x,q) \simeq \tilde{\mathcal{G}}(0,q)\frac{K'}{1+K'}C_0\exp[-\frac{1}{2}(\delta_R+\delta_P)q^2x]$ at zeroth order. In particular, it is impossible to access kinetics in the present approach when $\delta_R=\delta_P$.

Both preceding situations can be used to derive the thermodynamic features of the reaction (2) by analyzing either the relative amplitudes of the biexponential decay (slow $\mathbf{R} \rightleftarrows \mathbf{P}$ exchange regime) or the average apparent diffusion coefficient (fast $\mathbf{R} \rightleftarrows \mathbf{P}$ exchange regime). Note that the former case is more informative than the latter one as it does not rely on any *a priori* knowledge of the **R** and **P** diffusion coefficients.[1] Nevertheless, none of these two simplifying situations is appropriate to reach the kinetic information contained in the $\kappa_1+\kappa_2$ term.[6]

To progress in the identification of appropriate experimental conditions to extract the kinetic information from observing diffusion, one may notice from Eqs.(15) that, in the slow exchange regime, both eigenvalues, λ_+ and λ_-, do not contain the $\kappa_1+\kappa_2$ term

[6] In the slow exchange regime, the amplitude ratio gives only access to the ratio $\frac{\kappa_1}{\kappa_2}$, which depends on K'.

at leading order ($\lambda_+ \approx -\delta_P q^2$ and $\lambda_- \approx -\delta_R q^2$). In contrast, λ_- does contain the kinetic information at leading order in the fast exchange regime ($\lambda_+ \approx -\frac{1}{2}(\delta_P + \delta_R)q^2$ and $\lambda_- \approx -(\kappa_1 + \kappa_2)$). However, using Eqs.(21) and (23), we see that the associated amplitudes R_- and P_- scale as $\frac{(\delta_R - \delta_P)q^2}{\kappa_1 + \kappa_2}$, which is a very small term. In fact, the preceding asymptotic regimes suggest the $(\kappa_1 + \kappa_2) \approx (\delta_R - \delta_P)q^2$ regime to be the more appropriate to evidence kinetics by observing the spatial evolution of the diffusion profiles.[7] Indeed, both eigenvalues, λ_+ and λ_-, then equally depend on chemistry and diffusion. Moreover, the corresponding amplitudes, R_+ and R_- on one hand and P_+ and P_- on the other hand, exhibit balanced values because λ_+ and λ_- are at the closest in this regime (see Eqs.(20–23)).

Under the above defined conditions, one also has to take into account the concentration terms present in Eqs.(20–23). In particular, one should chose an appropriate concentration in $\mathcal{R}$ to fix K' as close as possible to one. In fact, the $K' = 1$ value is optimal to simultaneously get similar amplitudes associated to the λ_+ and λ_- eigenvalues, and thus to be able to extract the dynamic parameters sought for.[8]

[7] It is worth noting here that changing the applied voltage driving solutes motion is useful to access a suitable and large enough collection of spatial frequencies.

[8] Those conclusions are not markedly modified in the general case where Eqs.(16–19) rule the amplitudes of the exponential decays.

References

[1] A. Estévez-Torres, C. Gosse, T. Le Saux, J.- F. Allemand, V. Croquette, H. Berthoumieux, A. Lemarchand, L. Jullien, *Anal. Chem.*, **2007**, *79*, 8222-8231.